Cheatgrass / Downy brome

***Bromus tectorum* L. (Poaceae)**

Phenology/Degree-Day and Climate Suitability Model Analysis for USPEST.ORG

Prepared for USDA APHIS PPQ and USDA NIFA

Version 1.0 Aug. 2026

Brittany Barker and Len Coop

Department of Horticulture and Oregon Integrated Pest Management Center

Oregon State University

Summary

A phenology model and climate suitability model for *Bromus tectorum* L. (BRTE), known as cheatgrass or downy brome, was developed for the DDRP (Degree-Days, Risk, and Pest event mapping; under development for uspest.org) platform using data from available literature and from presence records in online biodiversity databases. DDRP was adapted for plants by replacing insect life stages with major plant phenophases (seed, seedling, flower, and mature) and incorporating antecedent soil moisture into the degree-day framework through a daily moisture modifier based on the cumulative vertical soil moisture gradient. The climatic suitability component was also expanded to include dry and wet soil moisture stresses alongside cold and heat stress, enabling predictions that account for both temperature and moisture limitations.

1. Introduction

Bromus tectorum L., commonly known as cheatgrass or downy brome (hereafter, BRTE), is a winter annual grass native to Eurasia that has invaded millions of acres of the western U.S., with isolated infestations occurring throughout the eastern U.S. First reported in Pennsylvania around 1790, BRTE became widely established throughout the U.S. between 1860 and 1900 and is now considered to be the most destructive exotic plant invader in the North American Intermountain West (Morrow and Stahlman 1983, Knapp 1996), where it infests more than 100 million acres of rangelands (Novak and Mack 2001, Bartlett et al. 2002). The weed has become a dominant part of the vegetation community in semi-arid regions, particularly in areas where native vegetation has been severely disturbed by grazing, fire, or cultivation (Hulbert 1955, Chambers et al. 2014). Infestations negatively impact the productivity of winter wheat, pastureland, alfalfa, grass seed fields, and rangelands, with an estimated reduction of 28% and 92% in small grain crop production systems (Rydrych and Muzik 1968, Stahlman and Miller 1990). The weed drastically shortens the natural fire return interval by producing flammable biomass (Brooks et al. 2004, Balch et al. 2013), resulting in more than US $20 million spent annually for rangeland fire management (Knapp 1996).

The objective of this study was to develop a phenology model and climate suitability model for BRTE for the DDRP (Degree-Days, Risk, and Pest event mapping) platform using data from available literature and from presence records in online biodiversity databases. The DDRP

platform was originally developed to predict climatic suitability (establishment risk) and phenology for insects, including invasive pests, biological control agents, and IPM species (Barker et al. 2020, 2023, 2025). We extended the platform to model plant phenology and climatic suitability using BRTE as a study system. Major modifications included (1) replacing insect life stages (egg, larva, pupa, and adult) with plant phenophases (seed, seedling, flower, and mature); (2) incorporating a moisture-modified degree-day model to account for the effects of soil moisture on plant development; (3) integrating cold, heat, dry, and wet stress indices for climatic suitability, rather than relying solely on temperature-based stresses; and (4) adding the capability to import and process soil moisture datasets required to model both phenology and climatic suitability. We then evaluated the extent to which including moisture modifications improved DDRP model predictions of flowering, seed set, and senescence using available monitoring datasets.

2. Methods

2.1. Study system

2.1.1. Environmental factors affecting BRTE's distribution

BRTE is adapted to semi-arid and arid environments receiving approximately 6–22 inches (150–560 mm) of annual precipitation, where most moisture occurs during fall and winter followed by dry summers (Hull and Pechanec 1947, Klemmedson and Smith 1964). In the absence of perennial herbaceous species, establishment, growth, and reproduction are greatest on warm, xeric sites and lowest on cold, mesic uplands (Chambers et al. 2007). Establishment generally increases during wetter years (Miller et al. 2006), whereas prolonged drought in late summer or early fall can reduce seedling survival (Mack and Pyke 1984, Rasmuson 1996). BRTE is less dominant in regions with high summer precipitation or persistently wet conditions, yet intense summer heat and episodic drought can also limit populations despite the species' tolerance of temperatures exceeding 40 °C (Warg 1938, Mack and Pyke 1983, Garbowski et al. 2021). Experimental work indicates that water additions can substantially increase BRTE's establishment rates (Miller et al. 2006), although waterlogged soil can induce seed mortality (Comes et al. 1978).

The northern distribution of BRTE in western North America closely corresponds to the −30 °C minimum winter temperature isocline (Mack 1981, Valliant et al. 2007). Because seed banks are short-lived, repeated lethal freezing events likely prevent long-term population persistence (Bykova and Sage 2012). Although snowpack can influence germination and overwinter survival, most seed mortality between November and March appears to result from winter conditions or other non-snow factors (Gornish et al. 2015).

2.1.2. Life cycle and environmental drivers of development

The phenological development of BRTE is strongly regulated by moisture availability. Seeds lose dormancy through dry after-ripening during summer and become capable of germinating when adequate soil moisture is available, although they may persist in the soil seed bank for more than one year (Wicks 1997, Smith et al. 2008). Germination typically occurs in fall or

winter following precipitation, with seedling emergence often triggered by *ca.* 5 cm of concentrated autumn rainfall or, alternatively, by snowmelt or seasonal rains in spring (Hull and Pechanec 1947, Klemmedson and Smith 1964, Mack and Pyke 1983, 1984, Pierson et al. 1990). Like other winter annuals, BRTE cohorts consist of individuals that lose innate dormancy (Hulbert 1955) and germinate during the intervals between autumn rainfall events. The timing and spread of cohort emergence are influenced by the frequency and magnitude of precipitation, as well as seed burial depth (Mack and Pyke 1983, 1984). Seedling growth declines rapidly under drought, with growth substantially reduced after 10 days without water, wilting occurring after 12 days, and development ceasing after approximately 15 days (Warg 1938, Zelikova et al. 2013).

Young plants overwinter as dormant rosettes and resume growth early the following spring, continuing development until soil moisture becomes limiting (Hull and Pechanec 1947, Klemmedson and Smith 1964). Plants subjected to drought or warmer-than-average spring temperatures rapidly shifted resources into flowering, which shortens the vegetative growing season but may allow for viable seed production even under significant environmental stress (Howell et al. 2020). Monitoring studies have found that seeds matured earlier under warmer, drier conditions (Hulbert 1955, Kray et al. 2025). In contrast, consistently wet habitats or prolonged rainfall and humidity can slow plant development, ultimately delaying senescence (Link et al. 1990, Zelikova et al. 2013, Prevéy and Seastedt 2014). In general, the flowering phase lasts 7–10 days, and mature, viable seeds are produced 1–4 weeks after flowering begins. During this period, the foliage and seed heads turn a distinct reddish-purple ("purple") color as the plant dries and transitions to maturity. Seeds become viable right when plants start turning purple and begin dropping off the plant shortly after the purple stage peaks. Within 1 to 4 weeks after seed maturity, plants have turned brown (brown stage) as whole-plant senescence and death occurs, during which most mature seeds are shed and dispersed.

2.2. Adapting DDRP for plant modeling

DDRP was originally developed to predict the timing of major insect life stages (egg, larva, pupa, and adult), together with a separately parameterized overwintering stage (e.g., an overwintering larva). To adapt DDRP for plants, we replaced insect life stages with major plant phenophases (seed, seedling, flower, and mature) commonly used in plant phenology models. The original temperature-driven degree-day framework was further modified to incorporate antecedent soil moisture by applying a daily moisture modifier derived from the cumulative vertical soil moisture gradient, thereby integrating moisture conditions preceding phenological development (see Section 2.5.3). Soil moisture was included because it influences developmental rates in annual plants. Higher soil moisture can delay flowering by prolonging vegetative growth, whereas drying conditions can accelerate flowering as part of a drought-escape response (Geber and Dawson 1990, Munson and Long 2017, Dai et al. 2022).

As with insect models, DDRP for plants uses time-distributed cohorts to represent variation in the timing of overwintering stage completion (Barker et al. 2020). Degree-day accumulation and phenophase transitions are simulated independently for each cohort, beginning when the overwintering stage completes development. Individuals within a cohort are assumed to develop synchronously. Models typically applied seven cohorts to approximate a normal distribution of development completion times and to allow for reasonable model run times since the phenology

model is run separately for each cohort. The resulting plant version of DDRP produces the same suite of outputs as previous insect implementations, including maps of phenophases present, dates of phenological events (e.g., flowering and seed production), and the number of generations.

The climatic suitability component of DDRP was also extended to incorporate soil moisture. Dry and wet stress accumulations were added so that cold, heat, dry, and wet stresses are jointly considered when predicting potential distribution. Daily soil moisture data are imported into DDRP, and moisture stress accumulates whenever soil moisture falls below or exceeds user-defined dry and wet stress thresholds, respectively. Moisture stresses are calculated using the same cumulative framework as temperature stresses, except that daily stress units are multiplied by 100 because soil moisture is expressed as volumetric water content (water volume/total soil volume), which would otherwise produce fractional stress values.

DDRP compares cumulative climate stress values with user-defined moderate and severe stress limits to delineate areas suitable for establishment (Barker et al. 2020). Moderate stress indicates conditions that may limit long-term establishment, although short-term establishment may occur during favorable years, whereas severe stress is assumed to preclude even short-term establishment. Areas excluded by moderate stress are also excluded by severe stress. For BRTE, dry and wet moisture stresses were incorporated using the same cumulative stress framework previously developed for cold and heat stress, whereby daily moisture stress accumulations are compared with moderate and severe stress limits to identify locations where moisture availability is expected to limit establishment. As in the original DDRP implementation, identical climate stress thresholds and limits are assumed across life stages, and recovery between episodes of stress accumulation is not modeled (Barker et al. 2020).

2.3. Climate data

For near real-time modeling for CONUS, we run DDRP using daily minimum and maximum temperature (T_{min} and T_{max}, respectively) data for the contiguous U.S. (CONUS) at 4-km resolution from the PRISM database (available at https://prism.oregonstate.edu) (Daly et al. 2008). Forecasts through the end of the calendar year are generated using daily-downscaled NMME (North American Multi-Model Ensemble) 7-month forecasts (Kirtman et al. 2014) combined with bi-monthly updated 10-year average temperatures. However, we used daily estimates of T_{min} and T_{max} from the Daymet database (1-km resolution; available at https://daymet.ornl.gov/getdata) (Thornton et al. 2021) for calibrating the climatic suitability model for BRTE in order to include the coldest regions of the weed's range in North America (southern Canada). Daymet data were aggregated from 1-km to 4-km resolution to decrease model run times.

For near real-time modeling, we used NASA's Soil Moisture Active Passive (SMAP) Level-4 Soil Moisture data product (Reichle et al. 2017, 2019) to obtain daily estimates of surface (0–5 cm) and root zone (0–100 cm) soil moisture at 9-km resolution. Forecasts through the end of the calendar year are generated using bi-monthly updated 10-year average soil moisture. Root zone estimates are appropriate for BRTE because plants typically reach rooting depths of 50 to 130 cm by flowering time (Hulbert 1955, Harris 1967), enabling them to extract moisture efficiently from much of the upper soil profile, with water depletion reported to depths of approximately 70 cm (Howell et al. 2020). However, soil moisture depletion is generally greatest in the upper 30–

40 cm of the profile, particularly in dense BRTE stands (Cline et al. 1977). Surface soil moisture (0–5 cm) captures short-term fluctuations associated with recent rainfall and evaporation, providing an indicator of immediate moisture availability near the soil surface. SMAP data were aggregated to 4-km to match the spatial resolution of the temperature datasets.

2.4. Observations used for model calibration and validation

Phenological observations from four published studies (Howell et al. 2020, Prevéy et al. 2024, Kray et al. 2025, Vahsen et al. 2025) and one unpublished dataset (Kray and Blumenthal, pers. commun.) spanning Arizona, Colorado, Idaho, Nebraska, Utah, and Wyoming were used to calibrate and validate the phenology model (Fig. 1; Appendix A). Multi-year datasets (2–4 years) were used for model calibration, whereas independent single-year datasets were reserved for validating flowering and senescence predictions, yielding 90 calibration observations and 32 validation observations (Table 1). Because observations of 50% flowering and seed set were limited, these phenophases were used only for calibration. The dataset of Vahsen et al. (2025) included multiple genotypes grown in common gardens; therefore, we used the median date of each phenological event for each garden. Following Vahsen et al. (2025), green, purple, and brown plant stages were classified as flowering, seed set, and senescence, respectively. For Howell et al. (2020), only observations from the control plots of the experimental warming study were included.

The climatic suitability model was developed using eco-physiological information and presence records that spanned areas of BRTE's range with the lowest T_{min} (parts of Canada), the highest T_{max} (the southwestern U.S.), the lowest soil moisture (the southwestern U.S. and the Great Basin), and the highest soil moisture (Great Lakes region and eastern Canada). Records were derived from the Global Biodiversity Information Facility (GBIF.org 2025) and EDDMapS (EDDMapS 2024). Duplicate records, GBIF records with a geographic uncertainty of >10 km, and records that occurred outside of climate grid cells were excluded. The resulting dataset of 43,068 records was randomly partitioned into calibration (75%) and validation (25%) datasets.

2.5. Phenology model

2.5.1 Thresholds, stage durations, and phenological events

We applied a lower and upper developmental threshold of 0 °C and 35 °C, respectively, for all major phenophases of BRTE in the model. A lower developmental threshold (LDT) of 0 °C as used in a previous degree-day model for BRTE (Ball et al. 2004) and field and laboratory studies indicated that germination occurs only after air and soil temperatures were ≥ 0 °C (Evans and Young 1972, Mack and Pyke 1984). An upper developmental temperature threshold of 35 °C was applied based on a sharp decline in average growth rates observed between 35 and 40 °C (McCarlie et al. 2001). The model applies the single triangle calculation method with upper threshold to calculate degree-days, uses a start date of January 1, and assumes a one-year life cycle in which the seedling is the overwintering stage. Although BRTE overwinters as a rosette or tuft rather than a true seedling, the model refers to this stage as seedling for simplicity.

The phenology model predicts the onset of seed dormancy (beginning of the seed stage), first flowering (end of the seedling stage), seed set (end of the flower stage), and senescence (end of

the mature stage). To our knowledge, thermal requirements for these life stages have not been quantified experimentally for BRTE. We therefore used estimates from a 2-year monitoring study conducted at two Pacific Northwest locations, which reported cumulative thermal requirements of 800, 200, and 350 DDC (LDT = 0 °C) for panicle (seedhead) emergence, seed set, and physiological maturity, respectively (Ball et al. 2004). Preliminary model runs showed that applying the 800-DDC threshold to first flowering consistently overpredicted flowering dates in the calibration dataset. Because first flowering occurs during and primarily after panicle emergence, we treated Ball et al.'s (2004) estimate as an initial reference value and calibrated the flowering threshold by testing values from 300 to 500 DDC in 25-DDC increments. After identifying the degree-day thresholds that best predicted first flowering, we evaluated whether incorporating soil moisture further improved predictions of this and events for subsequent stages (Section 2.5.2). Next, the reported degree-day requirements for physiological maturity were likewise used as starting values and refined using the calibration dataset. The duration of the flower stage (i.e., flowering to seed set) was set to 175 DDC, which corresponds to the difference between physiological maturity and seed set (i.e. 350 – 200 DDC) estimated by Ball et. (2004).

Prediction error for phenological events was estimated as the difference between the predicted day-of-year (DOY) of first flowering to the observed DOY for each flower observation in the calibration dataset. Predictive performance was evaluated using the mean absolute error (MAE), root mean square error (RMSE), prediction bias, and mean within-site standard deviation (SD) of prediction error across years. MAE quantified the average magnitude of prediction error, RMSE emphasized larger errors, bias assessed systematic over- or under-prediction, and the mean within-site SD measured the interannual consistency of predictions at individual locations. The degree-day requirements for was selected by prioritizing low MAE and mean within-site SD, with RMSE and prediction bias used as complementary diagnostics to evaluate large errors and systematic bias.

Calibration observations represented only the first occurrence of each phenological event and therefore corresponded to the earliest cohort in the model (parameter "xdist1"). The "distro_mean" parameter, representing the average degree-day requirement for seedlings to reach 50% flowering, was calibrated using 10 observations of ≥50% flowering from Nebraska and Wyoming (Kray et al. 2025, Kray and Blumenthal, pers. commun.). Because insufficient observations were available to estimate the upper limit of the cohort distribution, the "xdist2" parameter was set such that the interval between "distro_mean" and "xdist2" equaled the interval between "xdist1" and "distro_mean" (130 DDC).

2.5.2. Evaluation of soil moisture effects on flowering predictions

To identify soil moisture conditions associated with flowering in BRTE, daily soil moisture trajectories from observations in the calibration dataset for the phenology model were aligned by observed flowering date. For each of 38 site-years, the flowering date was designated as Day 0, and preceding observations were expressed as negative values representing days before flowering (e.g., −30 to 0 days). This event-based alignment enabled soil moisture dynamics from multiple years to be compared on a common developmental timescale despite interannual variation in flowering date. Three daily moisture metrics were evaluated: (1) surface soil moisture, (2) root-zone soil moisture, and (3) the vertical soil moisture gradient, calculated as root-zone soil moisture minus surface soil moisture. The gradient was included to characterize

the vertical distribution of soil water and the progression of seasonal drying through the soil profile, with positive values indicating wetter subsurface soils than surface soils and therefore greater access to deeper soil moisture as surface soils dry.

Aligned trajectories from all site-years were analyzed separately for each moisture metric using linear regression to quantify the relationship between antecedent soil moisture and flowering timing (or flowering model residuals). We evaluated candidate antecedent periods of 7, 14, 21, 28, 35, and 42 days preceding flowering. For each window, the cumulative antecedent surface soil moisture, root-zone soil moisture, and soil moisture gradient (root-zone minus surface soil moisture) were quantified as the area under the daily moisture curve (AUC) using the trapezoidal rule. Separate linear regression models were fit for each moisture metric, and model performance was compared using R-squared (R^2), Akaike's Information Criterion (AIC), and the RMSE. The antecedent period and moisture metric that maximized R^2 while minimizing AIC and RMSE were selected for subsequent analyses. Because the 35-day cumulative antecedent root-zone minus surface soil moisture gradient provided comparable explanatory power while representing the shortest antecedent period (see Results), it was selected for subsequent analyses.

To determine whether antecedent soil moisture explained residual variation in the temperature-only flowering model, a linear regression was fit with flowering prediction error (predicted flowering date − observed flowering date) as the response variable and the 35-day cumulative antecedent root-zone minus surface soil moisture gradient (AUC) as the predictor. This analysis tested whether incorporating antecedent soil moisture conditions could explain systematic prediction error remaining after accounting for temperature-driven phenological development.

2.5.3. Moisture-modified degree-day model

The moisture-modified degree-day model incorporated the cumulative 35-day antecedent soil moisture gradient (AUC) as a correction to the temperature-based flowering prediction. At each location and time step, DDRP calculated the antecedent AUC and applied the resulting moisture adjustment to the predicted first flowering date (i.e., for the first cohort), allowing forecasts to account for the influence of antecedent soil moisture. For each simulation day (t), the daily soil moisture gradient was calculated as:

$$G_t = \theta_{r,t} - \theta_{s,t}$$

where G_t is the daily soil moisture gradient, $\theta_{r,t}$ is volumetric soil moisture in the root zone, and $\theta_{s,t}$ is volumetric soil moisture in the surface soil layer. Antecedent moisture conditions were represented by the 35-day cumulative soil moisture gradient according to following equation:

$$C_t = \sum_{i=t-34}^{t} G_i$$

where C_t is the cumulative soil moisture gradient over the previous 35 days (i.e., the 35-day area-under-the-curve metric calculated as a running sum of daily moisture gradients). Daily degree-day accumulation was modified according to the following equation:

$$M_t = \exp[-k(C_t - C_{ref})]$$

where M_t is the moisture modifier, k is the moisture sensitivity coefficient that determines the magnitude of the phenological response to departures from the reference moisture condition, and C_{ref} is the reference cumulative antecedent soil moisture gradient for which $M_t = 1$, such that no adjustment is applied when antecedent moisture is average, whereas drier and wetter conditions respectively increase or decrease daily degree-day accumulation according to the moisture modifier. Larger values of k produce progressively greater acceleration of development under drier-than-average conditions and greater deceleration under wetter-than-average conditions.

To calibrate the moisture modifier, we evaluated the performance of the DDRP phenology model across a range of values for k. Candidate values ranging from 0.20 to 0.60 in increments of 0.05. Values outside this range were excluded because preliminary analyses consistently resulted in poorer model performance, including higher MAE, RMSE, prediction bias, and mean within-site SD of prediction error across years. The optimal value of k was selected by prioritizing low MAE and mean within-site SD, with RMSE and prediction bias used as complementary diagnostics to evaluate large errors and systematic bias.

Moisture-adjusted daily degree-day accumulation was then calculated as:

$$DD_t = DD_t \times M_t*$$

where DD_t is the unadjusted daily degree-day accumulation. Adjusted degree-days were accumulated through time until the developmental threshold for flowering was reached because the moisture modifier increased error for predictions of senescence and no significant relationship existed between prediction error and the antecedent soil moisture gradient for seed production or senescence (see Results).

2.6. Climate suitability model

2.6.1. Climate analysis of presence records

To identify thresholds for cold, heat, dry, and wet stress, we characterized the climate associated with all BRTE presence records used to calibrate the climatic suitability model. Climate data included Daymet daily temperature estimates (2004–2025) and SMAP daily soil moisture estimates (2015–2025). For each candidate threshold and presence record, we calculated the duration of consecutive days per year during which temperature was below (cold stress) or above (heat stress) the threshold, or soil moisture was below (dry stress) or above (wet stress), and then averaged durations across years. Candidate thresholds ranged from −34 to −20 °C for cold stress and 34 to 45 °C for heat stress (1 °C increments), 0.01 to 0.07 $m^3\ m^{-3}$ for dry stress (0.01 $m^3\ m^{-3}$ increments), and 0.50 to 0.95 $m^3\ m^{-3}$ for wet stress (0.05 $m^3\ m^{-3}$ increments below 0.90 and 0.01 increments thereafter). Root-zone moisture was used for climatic suitability modeling because BRTE rapidly develops a deep taproot after germination, making it a more

biologically relevant indicator of water availability than surface soil moisture (Hulbert 1955, Sauer et al. 1984).

2.6.2. Temperature stress parameters

The model applied a cold stress threshold of –32 °C based on laboratory studies demonstrating the freezing tolerance of BRTE from southwestern Saskatchewan, Canada (O'Connor et al. 1991, Bykova and Sage 2012). Although the climate analysis indicated no presence records from areas experiencing consecutive days with $T_{min} \leq -23$ °C (Fig. 2), a field study reported only slight leaf injury when ground surface temperatures dropped to as low as −23 °C (Hulbert 1955). These findings suggest that a cold stress threshold of −23 °C would underestimate the cold stress threshold of BRTE. We used a heat stress threshold of 44 °C because only two presence records occurred in areas that experienced consecutive days with $T_{max} \geq 44$ °C (Fig. 2). The cold and heat stress limits were calibrated to minimize the number of records excluded by stress accumulation. Where possible, we verified the presence status of BRTE in areas experiencing high levels of climatic stress to ensure the selected thresholds were not overly permissive, resulting in overprediction of the potential distribution. For example, a few records from the hottest parts of the southwestern United States were considered potential misidentifications of *Bromus rubens* L., a closely related species that closely resembles BRTE during early growth stages.

2.6.3. Moisture stress parameters

The model applied dry- and wet-stress thresholds of 0.02 and 0.92 $m^3\ m^{-3}$, respectively, because no presence records occurred in areas experiencing multiple days below or above these thresholds (Fig. 2). The dry-stress threshold was also set below the estimated permanent wilting point for BRTE, which occurs at approximately 3–14% volumetric soil moisture in the coarse-textured soils where the species is most abundant, to represent conditions likely to cause mortality rather than temporary water stress (Sauer et al. 1984, Werle et al. 2014, Moler et al. 2022). Calibration of the dry- and wet-stress thresholds followed the same approach used for temperature stresses.

2.6.4. Climatic suitability model validation

The performance of the climatic suitability model was evaluated by comparing annual predictions of climatic suitability with independent presence records in the validation dataset. DDRP was run for each year from 2016 to 2025, and the predicted potential distribution (areas not excluded by cold, heat, dry, or wet stress) was extracted for each presence location. Model performance was quantified as the number of years in which each presence record in the validation dataset was correctly predicted to be climatically suitable.

2.7. Model demonstration

To illustrate DDRP model outputs for BRTE, we generated maps of predicted first flowering and first senescence across the western U.S. for 2024 using daily PRISM temperature and SMAP soil moisture data as climate inputs. We selected 2024 because it was the warmest year on record

for both the western U.S. and CONUS, providing an example of phenological responses under temperatures that may become increasingly common under future climate conditions. The maps also incorporated estimates of the potential distribution based on the combined effects of cold, heat, dry, and wet climatic stresses.

3. Results

The final DDRP model is shown in Table 2.

3.1. Phenology model

3.1.1. Evaluation of soil moisture effects on flowering predictions

The antecedent soil moisture gradient (root-zone minus surface soil moisture) consistently explained more variation in flowering prediction error than either root-zone or surface soil moisture alone (Table 3). Linear regression models based on the 35- and 42-day antecedent windows produced the highest R^2 values and the lowest AIC and RMSE values among all candidate models, indicating that moisture redistribution within the soil profile during the five to six weeks preceding flowering was more strongly associated with flowering timing than moisture in either soil layer alone. Because the 35-day model was statistically indistinguishable from the 42-day model (ΔAIC < 1; ΔRMSE < 0.1 day), the 35-day window was selected for subsequent analyses (Fig. 3). Incorporating this 35-day antecedent soil moisture gradient into the moisture-modified degree-day model substantially improved flowering predictions, increasing the explained variation from 13% to 58% (R^2 = 0.13 vs. 0.58), reducing RMSE from 20.0 to 13.9 days, and lowering AIC from 342 to 314 relative to the temperature-only model. A nested model comparison confirmed that inclusion of the antecedent soil moisture gradient significantly improved model fit (ANOVA: F = 54.2, P < 0.0001), demonstrating that the vertical distribution of soil water captures an important component of flowering phenology not explained by temperature alone.

In contrast, extending the moisture-modified degree-day model beyond flowering did not improve predictions of senescence. Applying the moisture modifier after flowering explained the same proportion of variation in observed senescence dates (R^2 = 0.58, AIC = 550, RMSE = 11 days) as the unmodified model (R^2 = 0.58, AIC = 548, RMSE = 11 days), and a nested model comparison confirmed no significant improvement in model fit (ANOVA: F = 2.4, P = 0.12). The 28- and 42-day antecedent windows performed similarly to the 35-day window, indicating that alternative accumulation periods would not improve predictions. Together, these results suggest that antecedent soil moisture primarily influences the timing of flowering, with limited additional benefit for modeling subsequent developmental stages.

3.1.2. Moisture-modified degree-day model

The reference cumulative antecedent soil moisture gradient (C_{ref}) was estimated as the mean 35-day antecedent AUC across all calibration site-years (C_{ref} = 0.91). This value closely corresponded to the point at which the regression of flowering prediction error on antecedent soil

moisture crossed zero (Fig. 3), representing the moisture condition under which the temperature-only model was, on average, unbiased. Among the candidate values of the moisture sensitivity coefficient, $k = 0.40$ produced the lowest MAE, while maintaining a similar RMSE, lower prediction bias, and nearly the lowest mean within-site SD of prediction error compared with the next-best value ($k = 0.45$; Table 4). We therefore selected $k = 0.40$ for the final phenology model, providing the best overall balance of prediction accuracy, bias, and temporal consistency across years.

The phenology model predicted major BRTE phenophases with generally good accuracy (Table 5). MAE ranged from 9.9 days for 50% flowering to 15.5 days for first seed set in the calibration dataset, with RMSE values ranging from 11.5 to 19.7 days. Model performance was maintained during independent validation, with MAEs of 14.8 and 11.6 days and RMSEs of 16.6 and 13.8 days for first flowering and first senescence, respectively. Prediction bias was low for most phenophases, indicating little systematic tendency to predict events too early or too late, although first senescence was predicted an average of 5.3 days later than observed in the validation dataset.

3.2. Climate suitability model

The climatic suitability model correctly classified 99.8% (10,750 of 10,767) of validation presence records as occurring within the predicted potential distribution across North America during 2016–2025, indicating excellent model sensitivity. Across the 10-year period, BRTE was predicted to occur throughout most of CONUS and southern Canada (Fig. 4). Climatically unsuitable areas were largely confined to the coldest and wettest parts of Canada because of cold and wet stress accumulations (Fig. 5). In contrast, heat and dry stress excluded BRTE from only small portions of the Mojave and Sonoran deserts, while wet stress additionally limited suitability in the Great Lakes region and the Olympic Peninsula of Washington. Presence records for BRTE were absent or rare in some areas predicted to be suitable, such as much of the California Central Valley, southwestern Arizona, and western Oregon and Washington (Fig. 4).

3.3. Model demonstration

Predicted timing of first flowering and first senescence for BRTE across CONUS in 2024 varied markedly with latitude and elevation. In northern and high-elevation regions, first flowering occurred primarily between April and June, seed set occurred 1–3 weeks later, and first senescence occurring between June and August (Fig. 6). In contrast, flowering and senescence occurred approximately two months earlier in warmer regions, such as southern California and Arizona, where first senescence was predicted as early as February and March. The predicted average dates of flowering were *ca.* 1-2 weeks following first flowering. Areas excluded by climatic stress were limited to the hottest and driest portions of southern California and Arizona. Cold and wet stress did not exclude BRTE from any part of CONUS, indicating that climatic suitability was constrained almost entirely by extreme heat and aridity.

4. Discussion

4.1. Performance of a moisture-modified phenology model for plants

The antecedent soil moisture gradient provided greater explanatory power for predictive error in BRTE flowering than either root-zone or surface soil moisture alone. Because surface soils typically dry before deeper root zones, an increasing vertical soil moisture gradient may provide an early signal of impending water limitation, triggering physiological responses that accelerate flowering and reproduction as a drought-escape strategy (Kooyers 2015, Shavrukov et al. 2017, Tran et al. 2024). Conversely, a weaker or more stable gradient may indicate sustained access to soil water, promoting continued vegetative growth and delaying reproduction (Link et al. 1990, Prevéy and Seastedt 2014). Consistent with this interpretation, incorporating antecedent soil moisture into the phenology model substantially improved predictions of flowering, similar to findings for chickpea and wheat, where inclusion of soil moisture improved flowering-time predictions (Chauhan et al. 2019). More broadly, our results align with observations that flowering is delayed in many grass species under wetter conditions, as evidenced by later flowering with increasing mean annual precipitation across the western United States (Munson and Long 2017).

Extending the moisture-modified degree-day model beyond flowering did not improve predictive accuracy for later phenological stages, likely because water availability exerts its greatest influence during germination, vegetative growth, and the transition to flowering (Kooyers 2015, Shavrukov et al. 2017). By the time BRTE enters seed production and seed filling, soils in semi-arid ecosystems have often dried throughout the rooting profile (Thill et al. 1984, Chambers et al. 2014), causing the vertical soil moisture gradient to collapse into relatively uniform deep-soil drought. Consequently, variation in soil moisture is likely less influential on developmental rate during seed maturation than during earlier growth stages.

Although the SMAP Level-4 dataset incorporates soil texture and hydraulic properties when estimating root-zone soil moisture (Reichle et al. 2017, 2019), it does not represent many other edaphic characteristics that influence BRTE performance. Consequently, the modeled soil moisture should capture some differences in water availability among soil types (e.g., loam, clay, and sand) that affect BRTE growth and establishment (Miller et al. 2006), but it cannot represent differences in soil color, fertility, nutrient availability, or organic matter. These factors influence growth and phenology in annual *Bromus* species (Miller et al. 2006, Belnap et al. 2016, Maxwell et al. 2023, Vahsen et al. 2025) and may explain additional variation not captured by climate variables alone. Incorporating spatial information on these soil properties may therefore improve predictions of BRTE phenology and climatic suitability.

Model performance may also be constrained by the coarse spatial resolution of the SMAP soil moisture product (9 km). Individual pixels may encompass substantial variation in topography, vegetation cover, soil texture, and soil depth, all of which influence soil moisture at the microsite scale experienced by individual plants. Consequently, local variation in soil moisture cannot be fully resolved, even when the underlying environmental drivers are represented. Although higher-resolution soil moisture products, including a global 1-km downscaled SMAP dataset (Fang et al. 2024), have recently become available, they are not currently produced in near real-time and therefore cannot be incorporated into operational DDRP forecasts. Likewise, field-based soil moisture measurements, such as the volumetric probes used by Maxwell et al. (2023), would likely improve predictive accuracy but are impractical to obtain across the large spatial extents for which DDRP is designed.

4.2. Future opportunities to improve the phenology model

Environmental variables not currently represented in the model may further improve prediction accuracy. Future work could evaluate whether incorporating the Continuous Heat-Insolation Load Index (CHILI), which quantifies potential solar radiation based on topography and latitude, further improves model performance. Prevéy *et al.* (2024) found that including CHILI in phenology models for BRTE and *B. rubens* substantially improved model fit, reducing prediction error by approximately 7.5 days across phenophases. However, CHILI is closely related to soil moisture because warmer, more exposed sites generally experience greater evapotranspiration and more rapid soil drying. Consequently, CHILI and the antecedent soil moisture metrics used here may capture overlapping environmental variation, potentially limiting the additional predictive benefit of including both variables. Whether CHILI provides information beyond that already captured by soil moisture remains an important question for future study.

The current model does not incorporate photoperiod because its role in regulating BRTE flowering remains uncertain. Some studies have suggested that increasing spring day length promotes floral development and rapid seed production, potentially preventing premature flowering during the short days of autumn and winter (Finnerty and Klingman 1962, Pierson et al. 1990). However, Ball *et al.* (2004) argued that photoperiod is unlikely to be import for predicting reproductive phenology because development occurs under increasing day length throughout the species' latitudinal range, making photoperiod relatively invariant under natural conditions. Similarly, Prevey *et al.* (2024) found that incorporating photoperiod into a phenology model BRTE only reduced errors rates by *ca.* 1 and 3 days for flowering and senescence, respectively. These findings suggest that explicitly modeling photoperiod would likely provide only modest gains in predictive accuracy, although its contribution could be evaluated more rigorously in future studies. However, local variation in light availability may represent an unmodeled source of prediction error, as flowering was delayed by approximately 2–6 weeks in plants grown under 60–90% shade compared with those grown in full sunlight (Klemmedson and Smith 1964, Pierson et al. 1990).

Incorporating population-specific developmental thresholds or ecotype-specific parameterizations may further improve prediction accuracy across BRTE's geographic range. Genetically based variation in flowering phenology among populations has been widely documented, indicating substantial local adaptation across the western U.S. (Rice and Mack 1991, Hufft and Zelikova 2016, Gamba 2025, Vahsen et al. 2025). In one of the earliest common-garden studies, Hulbert (1955) found that plants from different geographic populations differed by up to approximately 25 days in inflorescence emergence and 20 days in senescence, despite being grown under the same environmental conditions. More recent common-garden experiments have shown that selection on flowering time reverses between warm and cold environments, potentially maintaining geographic clines in phenology (Gamba 2025). BRTE also exhibits phenotypic plasticity in response to environmental stress, with genetic variation in the degree of plasticity among populations (Moler et al. 2022). These findings suggest that developmental parameters, particularly the lower developmental threshold, may vary among populations. Consistent with this hypothesis, populations from the Great Basin exhibited greater variation in developmental responses at lower temperatures than at higher temperatures, indicating local adaptation of the lower developmental threshold (McCarlie et al. 2001).

The current model assumes autumn germination followed by seedling overwintering and therefore does not account for spring germination, which may occur when autumn moisture is insufficient (Stewart and Hull 1949, Hulbert 1955). Spring-germinating plants may exhibit different developmental trajectories than autumn-germinating plants. For example, Finnerty and Klingman (1962) reported that plants germinating after April 1 often exhibited a biennial life history, producing seed the following spring rather than during the year of germination. The model also does not account for the potential effects of vernalization, the promotion of flowering by prolonged exposure to cold temperatures. Evidence for a vernalization requirement in BRTE is mixed. Hulbert (1955) found that plants established after late March failed to flower, suggesting a requirement for winter chilling, but also observed that spring-planted individuals could reach the flowering stage, indicating that vernalization is not obligatory.

Future model development could incorporate prediction of fall germination and seedling emergence. However, modeling seed dormancy loss and germination is considerably more complex than modeling post-emergence phenology because germination is regulated by interacting effects of temperature, soil moisture, after-ripening, seed bed type, and seed age. During the warm, dry conditions of summer, seeds gradually lose dormancy through after-ripening, typically becoming capable of germinating after 4–12 weeks (Hulbert 1955, Wicks 1997, Smith et al. 2008). Germination typically occurs following autumn or winter precipitation when adequate soil moisture is available, whereas high summer temperatures inhibit germination even after rainfall (Hulbert 1955, Steinbauer and Grigsby 1957, Mack and Pyke 1983, 1984, Milby and Johnson 1987). As after-ripening progresses, seeds become capable of germinating over a broader temperature range (up to approximately 30 °C), and the inhibitory effects of light decline as they fall beneath surface litter, increasing the likelihood of germination (Hulbert 1955). Microsite conditions affect germination because of differences in soil temperatures at different depths that seeds may occur (Evans and Young 1972).

Experimental studies further demonstrate that after-ripening and germination rates depend on interactions between temperature and soil moisture, with warm, dry conditions regulating dormancy loss and soil moisture modifying temperature responses during germination (Bauer et al. 1998, Meyer and Allen 1999, Bair et al. 2006, Werle et al. 2014). Consequently, accurately predicting germination will likely require integrating surface soil moisture dynamics associated with precipitation events with temperature-dependent after-ripening and germination processes (Hulbert 1955, Harris 1977, Mack and Pyke 1984). Developing and validating such a model will require substantially more germination observations spanning multiple sites and years during the period of SMAP soil moisture availability, as we found only four germination observations from two sites for this period.

4.3. Climatic suitability model

The climatic suitability model predicted that most of CONUS was suitable for BRTE establishment during each modeled year (2016–2025), including areas where the species is rare or potentially absent. This apparent overprediction likely reflects biotic interactions that limit BRTE abundance rather than climatic constraints. For example, BRTE is uncommon in low-elevation deserts of the southwestern U.S., where it is largely replaced by *B. rubens*, which is better adapted to hotter, drier, and lower-elevation environments such as the Mojave Desert and California's Central Valley (Bykova and Sage 2012, Chambers et al. 2014). Similarly, dense

perennial vegetation and high winter and spring precipitation likely contribute to BRTE's rarity in parts of the Pacific Northwest despite suitable climatic conditions (Chambers et al. 2007, Bradley 2009).

The climatic suitability model also does not account for physiological and environmental processes that may enhance winter survival. For example, it does not represent cold acclimation, which substantially increases freeze tolerance in winter annuals and is critical for overwinter survival (Bykova and Sage 2012), nor does it account for the insulating effects of snow, which can maintain plant crowns and roots near 0 °C despite subfreezing air temperatures and permit seedling emergence throughout winter, with emergence observed as soon as one day after snowmelt (Mack and Pyke 1984). Future model development could also evaluate life-stage-specific climate stress accumulation, as heat and dry stress are most likely to reduce survival of recently germinated seedlings during autumn rather than established plants (Warg 1938, Zelikova et al. 2013).

4.4. Applications

The successful control of BRTE relies on predicting its phenology and establishment risk under both current and future climates (Howell et al. 2020, Garbowski et al. 2021, Prevéy et al. 2024). Forecasts of phenology can improve the timing and effectiveness of integrated pest management by identifying when key life stages occur. Because cattle consumption declines as plants mature and seeds ripen (Kray et al. 2025), forecasts of flowering can help managers optimize grazing before forage quality decreases. Flowering forecasts can also guide mowing, which is most effective for reducing seed production when conducted within one week after flowering (Fenster et al. 1970). Forecasts of seed set, when seeds are becoming viable, can help farmers and land managers schedule grazing, tillage, or herbicide applications to prevent replenishment of the soil seed bank (Fenster et al. 1970, Sebastian et al. 2017). Timely control is critical because delaying spring tillage or herbicide applications increases the likelihood of viable seed production during the fallow period, and failure to control plants before seed maturation can promote long-term persistence of infestations (Fenster et al. 1970, Sebastian et al. 2017). Forecasts of senescence also have important management value by identifying when cheatgrass has dried sufficiently to become highly flammable, increasing wildfire risk (Mack 1981, Brooks et al. 2004, Balch et al. 2013). These forecasts can support advance planning of fuel reduction measures, including mechanical removal and other vegetation management practices.

The DDRP model for BRTE could also be applied with future climate projections to assess potential shifts in phenology and climatic suitability under climate change. However, extending the moisture-modified model to future climates is currently constrained by the lack of projections for daily soil moisture, preventing direct simulation of the moisture effects incorporated in this study. This limitation is important because the response of BRTE to climate warming will depend strongly on moisture availability (Bradley 2009). The species has expanded rapidly throughout the Great Basin, invading higher elevations under recent warming, with tens of millions of acres remaining at high risk of invasion (Smith et al. 2022, Molvar et al. 2024). Continued range expansion is expected under warmer winters and springs, but projected responses are likely to vary with future precipitation and soil moisture conditions (Compagnoni and Adler 2014, Boyte et al. 2016, Bradley et al. 2016). Experimental studies further demonstrate that reduced precipitation can offset or even eliminate the positive effects of

warming on BRTE development, and warmer, drier winters may decrease survival (Zelikova et al. 2013, Gornish et al. 2015, Howell et al. 2020). Consequently, future applications of moisture-modified phenology models will likely require coupling climate projections with hydrologic or land-surface models capable of producing daily soil moisture estimates.

Acknowledgements

We thank Julie Kray, Megan Vahsen, Erika Geiger, Cara Lauria, and Daniel Winkler for assistance with obtaining phenology monitoring data for BRTE. This work was supported by awards from the USDA National Institute of Food and Agriculture (NIFA) Agriculture and Food Research Initiative (grant no. 2022-68013-37138), the USDA NIFA Crop Protection and Pest Management Extension Implementation Program (grant no. 2021-70006-35581), and the U.S. Department of Defense Strategic Environmental Research and Development Program (U.S. Army Corps of Engineers, contract no. RC23-3611).

Data availability

DDRP code used for modeling and Appendix A are available on GitHub at https://github.com/bbarker505/ddrp_plants.

References

Bair, N. B., S. E. Meyer, and P. S. Allen. 2006. A hydrothermal after-ripening time model for seed dormancy loss in *Bromus tectorum* L. Seed Science Research 16:17–28.

Balch, J. K., B. A. Bradley, C. M. D'Antonio, J. Gómez-Dans, W. Building, E. Analysis, S. Barbara, S. Barbara, J. K. Balch, B. A. Bradley, C. M. D'Antonio, J. Gómez-Dans, W. Building, E. Analysis, S. Barbara, S. Barbara, J. K. Balch, B. A. Bradley, C. M. D'Antonio, and J. Gómez-Dans. 2013. Introduced annual grass increases regional fire activity across the arid western USA (1980-2009). Global Change Biology 19:173–183.

Ball, D. A., S. M. Frost, and A. I. Gitelman. 2004. Predicting timing of downy brome (*Bromus tectorum*) seed production using growing degree days. Weed Science 52:518–524.

Barker, B. S., L. Coop, T. Wepprich, F. S. Grevstad, and G. Cook. 2020. DDRP: real-time phenology and climatic suitability modeling of invasive insects. PloS ONE 15:e0244005.

Bartlett, E., S. J. Novak, and R. N. Mack. 2002. Genetic variation in *Bromus tectorum* (Poaceae): Differentiation in the eastern United States. American Journal of Botany 89:602–612.

Bauer, M. C., S. E. Meyer, and P. S. Allen. 1998. A simulation model to predict seed dormancy loss in the field for *Bromus tectorum* L. Journal of Experimental Botany 49:1235–1244.

Belnap, J., J. M. Stark, B. M. Rau, E. B. Allen, and S. Phillips. 2016. Soil moisture and biogeochemical factors influence the distribution of annual *Bromus* species. Pages 227–256 *in* M. J. Germino, editor. Exotic Brome-Grasses in Arid and Semiarid Ecosystems of the Western US. Springer International Publishing, Switzerland.

Boyte, S. P., B. K. Wylie, and D. J. Major. 2016. Cheatgrass percent cover change: Comparing recent estimates to climate change - Driven predictions in the Northern Great Basin. Rangeland Ecology and Management 69:265–279.

Bradley, B. A. 2009. Regional analysis of the impacts of climate change on cheatgrass invasion shows potential risk and opportunity. Global Change Biology 15:196–208.

Bradley, B. A., C. A. Curtis, and J. C. Chambers. 2016. *Bromus* response to climate and projected changes with climate change. Pages 257–274 *in* M. J. Germino, J. C. Chambers, and C. S. Brown, editors. Exotic Brome-Grasses in Arid and Semiarid Ecosystems of the Western US. Springer.

Brooks, M. L., C. M. D'Antonio, D. M. Richardson, J. B. Grace, J. E. Keeley, J. M. DiTomaso, R. J. Hobbs, M. Pellant, and D. A. Pyke. 2004. Effects of invasive alien plants on fire regimes. BioScience 54:677–688.

Bykova, O., and R. F. Sage. 2012. Winter cold tolerance and the geographic range separation of *Bromus tectorum* and *Bromus rubens*, two severe invasive species in North America. Global Change Biology 18:3654–3663.

Chambers, J. C., B. A. Bradley, C. S. Brown, C. D'Antonio, M. J. Germino, J. B. Grace, S. P. Hardegree, R. F. Miller, and D. A. Pyke. 2014. Resilience to stress and disturbance, and resistance to *Bromus tectorum* L. invasion in cold desert shrublands of western North America. Ecosystems 17:360–375.

Chambers, J. C., B. A. Roundy, R. R. Blank, S. E. Meyer, and A. Whittaker. 2007. What makes Great Basin sagebrush ecosystems invasible by *Bromus tectorum*? Ecological Monographs 77:117–145.

Chauhan, Y. S., M. Ryan, S. Chandra, and V. O. Sadras. 2019. Accounting for soil moisture improves prediction of flowering time in chickpea and wheat. Scientific Reports 9:1–11.

Cline, J. F., D. W. Uresk, and W. H. Rickard. 1977. Comparison of soil water used by a sagebrush-bunchgrass and a cheatgrass community. Journal of Range Management 30:199–201.

Comes, R. D., V. F. Bruns, and A. D. Kelley. 1978. Longevity of certain weed and crop seeds in fresh water. Weed Science 26:336–344.

Compagnoni, A., and P. B. Adler. 2014. Warming, soil moisture, and loss of snow increase *Bromus tectorum*'s population growth rate. Elementa 2:000020.

Dai, W., Y. Yang, H. M. Patch, C. M. Grozinger, and J. Mu. 2022. Soil moisture affects plant-pollinator interactions in an annual flowering plant. Philosophical Transactions of the Royal Society B: Biological Sciences 377.

Daly, C., H. Halbleib, J. I. Smith, W. P. Gibson, M. K. Doggett, G. H. Taylor, J. Curtis, and P. P. Pasteris. 2008. Physiographically sensitive mapping of climatological temperature and precipitation across the conterminous United States. International Journal of Climatology 28:2031–2064.

EDDMapS. 2024. Early Detection & Distribution Mapping System. The University of Georgia - Center for Invasive Species and Ecosystem Health. Available online at: http://www.eddmaps.org (accessed on 10 December 2024).

Evans, R. A., and J. A. Young. 1972. Microsite requirements for establishment of annual rangeland weeds. Weed Science 20:350–356.

Fang, B., V. Lakshmi, and R. Zhang. 2024. Validation of downscaled 1-km SMOS and SMAP soil moisture data in 2010–2021. Vadose Zone Journal 23:e20305.

Fenster, C. R., G. A. Wicks, and L. R. Robiso. 1970. EC70-188 Know and control downy brome. Historical Materials from University of Nebraska-Lincoln Extension. 3980. https://digitalcommons.unl.edu/extensionhist/3980:1–11.

Finnerty, D. W., and D. L. Klingman. 1962. Life cycles and control studies of some weed bromegrasses. Weed Science 10:40–47.

Gamba, D. 2025. Local adaptation to climate has facilitated the global invasion of cheatgrass. Nature Communications 16:10203.

Garbowski, M., D. B. Johnston, D. V. Baker, and C. S. Brown. 2021. Invasive annual grass interacts with drought to influence plant communities and soil moisture in dryland restoration. Ecosphere 12:e03417.

GBIF.org. 2025. GBIF.org (1 October 2025) GBIF Occurrence Download https://doi.org/10.15468/dl.twmy4z.

Geber, M. A., and T. E. Dawson. 1990. Genetic variation in and covariation between leaf gas exchange, morphology, and development in *Polygonum arenastrum*, an annual plant. Oecologia 85:153–158.

Gornish, E. S., Z. T. Aanderud, R. L. Sheley, M. J. Rinella, T. Svejcar, S. D. Englund, and J. J. James. 2015. Altered snowfall and soil disturbance influence the early life stage transitions and recruitment of a native and invasive grass in a cold desert. Oecologia 177:595–606.

Harris, G. A. 1967. Some competitive relationships between *Agropyron spicatum* and *Bromus tectorum*. Ecological Monographs 37:89–111.

Harris, G. A. 1977. Root phenology as a factor of competition among grass seedlings. Journal of Range Management 30:172–177.

Howell, A., D. E. Winkler, M. L. Phillips, B. McNellis, and S. C. Reed. 2020. Experimental warming changes phenology and shortens growing season of the dominant invasive plant *Bromus tectorum* (cheatgrass). Frontiers in Plant Science 11:570001.

Hufft, R. A., and T. J. Zelikova. 2016. Ecological Genetics, Local Adaptation, and Phenotypic Plasticity in Bromus tectorum in the Context of a Changing Climate:133–154.

Hulbert, L. C. 1955. Ecological studies of *Bromus tectorum* and other annual bromegrasses. Ecological Monographs 25:181–213.

Hull, A. C., and F. Pechanec. 1947. Cheatgrass-a challenge to range research. Journal of Forestry 45:555–564.

Kirtman, B. P., D. Min, J. M. Infanti, J. L. Kinter, D. A. Paolino, Q. Zhang, H. Van Den Dool, S. Saha, M. P. Mendez, E. Becker, P. Peng, P. Tripp, J. Huang, D. G. Dewitt, M. K. Tippett, A. G. Barnston, S. Li, A. Rosati, S. D. Schubert, M. Rienecker, M. Suarez, Z. E. Li, J. Marshak, Y. K. Lim, J. Tribbia, K. Pegion, W. J. Merryfield, B. Denis, and E. F. Wood. 2014. The North American multimodel ensemble: Phase-1 seasonal-to-interannual prediction; phase-2 toward developing intraseasonal prediction. Bulletin of the American Meteorological Society 95:585–601.

Klemmedson, J. O., and J. G. Smith. 1964. Cheatgrass (*Bromus tectorum* L .). Botanical Review 30:226–262.

Knapp, P. A. 1996. Cheatgrass (*Bromus tectorum* L) dominance in the Great Basin Desert:

History, persistence, and influences to human activities. Global Environmental Change 6:37–52.

Kooyers, N. J. 2015. The evolution of drought escape and avoidance in natural herbaceous populations. Plant Science 234:155–162.

Kray, J. A., D. M. Blumenthal, M. B. Stephenson, L. M. Porensky, D. J. Augustine, S. J. Romero, M. C. Mortenson, and J. D. Derner. 2025. Using targeted grazing to close the phenological niche exploited by invasive annual bromes. Rangeland Ecology and Management 98:441–453.

Link, S. O., G. W. Gee, and J. L. Downs. 1990. The effect of water stress on phenological and ecophysiological characteristics of cheatgrass and Sandberg's bluegrass. Journal of Range Management 43:506–513.

Mack, R. N. 1981. Invasion of *Bromus tectorum* L. into western North America: an ecological chronicle. Agro-Ecosystems 7:145–165.

Mack, R. N., and D. A. Pyke. 1983. The demography of *Bromus tectorum*: variation in time and space. Journal of Ecology 71:69–93.

Mack, R. N., and D. A. Pyke. 1984. The demography of *Bromus tectorum*: the role of microclimate, grazing and disease. Journal of Ecology 72:731–748.

Maxwell, T. M., M. J. Germino, S. Romero, L. M. Porensky, D. M. Blumenthal, C. S. Brown, and P. B. Adler. 2023. Experimental manipulation of soil - surface albedo alters phenology and growth of *Bromus tectorum* (cheatgrass). Plant and Soil 487:325–339.

McCarlie, V. W., L. D. Hansen, and B. N. Smith. 2001. Respiratory and physiological characteristics in subpopulations of Great Basin cheatgrass. USDA Forest Service Proceedings RMRS-P-21.

Meyer, S. E., and P. S. Allen. 1999. Ecological genetics of seed germination regulation in *Bromus tectorum* L. I. Phenotypic variance among and within populations. Oecologia 120:27–34.

Milby, T. H., and F. L. Johnson. 1987. Germination of downy brome from southern Kansas, central Oklahoma, and north Texas. Journal of Range Management 40:534–536.

Miller, M. E., J. Belnap, S. W. Beatty, and R. L. Reynolds. 2006. Performance of *Bromus tectorum* L. in relation to soil properties, water additions, and chemical amendments in calcareous soils of southeastern Utah, USA. Plant Soil 288:1–18.

Moler, E. R. V, S. D. Zorio, and K. Aho. 2022. *Bromus tectorum* responses to intergenerational drought: Implications for evolvability and selection under climate warming. Weed Research 62:240–248.

Molvar, E. M., R. Rosentreter, D. Mansfield, and G. M. Anderson. 2024. Cheatgrass invasions: History, causes, consequences, and solutions. Hailey, ID: Western Watersheds Project, 128 pp.

Morrow, L., and P. Stahlman. 1983. The history and distribution of downy brome (*Bromus tectorum*) in North America. Weed Science Society of America 32:2–6.

Munson, S. M., and A. L. Long. 2017. Climate drives shifts in grass reproductive phenology across the western USA. New Phytologist 213:1945–1955.

Novak, S. J., and R. N. Mack. 2001. Tracing plant introduction and spread: genetic evidence from *Bromus tectorum* (cheatgrass). BioScience 51:114–122.

O'Connor, B. J., L. V. Gusta, and S. P. Paquette. 1991. A comparison of the freezing tolerance of downy brome, Japanese brome and Norstar winter wheat. Canadian Journal of Plant Science 71:565–569.

Pierson, E. A., R. N. Mack, and R. A. Black. 1990. The effect of shading on photosynthesis, growth, and regrowth following defoliation for *Bromus tectorum*. Oecologia 84:534–543.

Prevéy, J. S., I. S. Pearse, D. M. Blumenthal, A. J. Howell, J. A. Kray, S. C. Reed, M. B. Stephenson, and C. S. Jarnevich. 2024. Phenology forecasting models for detection and management of invasive annual grasses. Ecosphere 15:e70023.

Prevéy, J. S., and T. R. Seastedt. 2014. Seasonality of precipitation interacts with exotic species to alter composition and phenology of a semi-arid grassland. Journal of Ecology 102:1549–1561.

Rasmuson, K. E. 1996. Population and individual responses of *Bromus tectorum* to environmental stresses: a study of factors that may limit its distribution in cold desert habitats. PhD Dissertation, Idaho State University, Pocatello, ID.

Reichle, R. H., G. J. M. De Lannoy, Q. Liu, J. V. Ardizzone, A. Colliander, A. Conaty, W. Crow, T. J. Jackson, L. A. Jones, J. S. Kimball, R. D. Koster, S. P. Mahanama, E. B. Smith, A. Berg, S. Bircher, D. Bosch, T. G. Caldwell, M. Cosh, Á. González-Zamora, C. D. H. Collins, K. H. Jensen, S. Livingston, E. Lopez-Baeza, J. Martínez-Fernández, H. McNairn, M. Moghaddam, A. Pacheco, T. Pellarin, J. Prueger, T. Rowlandson, M. Seyfried, P. Starks, Z. Su, M. Thibeault, R. van der Velde, J. Walker, X. Wu, and Y. Zeng. 2017. Assessment of the SMAP Level-4 surface and root-zone soil moisture product using in situ measurements. Journal of Hydrometeorology 18:2621–2645.

Reichle, R. H., Q. Liu, R. D. Koster, W. T. Crow, G. J. M. De Lannoy, J. S. Kimball, J. V. Ardizzone, D. Bosch, A. Colliander, M. Cosh, J. Kolassa, S. P. Mahanama, J. Prueger, P. Starks, and J. P. Walker. 2019. Version 4 of the SMAP Level-4 Soil Moisture algorithm and data product. Journal of Advances in Modeling Earth Systems 11:3106–3130.

Rice, K. J., and R. N. Mack. 1991. Ecological genetics of *Bromus tectorum*. Oecologia 88:77–83.

Rydrych, D. J., and T. J. Muzik. 1968. Downy brome competition and control in dryland wheat. Agronomy Journal 60:279–280.

Sauer, R. H., M. L. Warner, and W. T. Hinds. 1984. Indirect determination of rooting depth and permanent wilting point. Ecological Modelling 21:109–124.

Sebastian, D. J., S. J. Nissen, J. R. Sebastian, and K. G. Beck. 2017. Seed bank depletion: the key to long-term downy brome (*Bromus tectorum* L.) management. Rangeland Ecology and Management 70:477–483.

Shavrukov, Y., A. Kurishbayev, S. Jatayev, V. Shvidchenko, L. Zotova, F. Koekemoer, S. De Groot, K. Soole, and P. Langridge. 2017. Early flowering as a drought escape mechanism in plants: How can it aid wheat production? Frontiers in Plant Science 8:1950.

Smith, D. C., S. E. Meyer, and V. J. Anderson. 2008. Factors affecting *Bromus tectorum* seed bank carryover in Western Utah. Rangeland Ecology and Management 61:430–436.

Smith, J. T., B. W. Allred, C. S. Boyd, K. W. Davies, M. O. Jones, A. R. Kleinhesselink, J. D.

Maestas, S. L. Morford, and D. E. Naugle. 2022. The elevational ascent and spread of exotic annual grass dominance in the Great Basin, USA. Diversity and Distributions 28:83–96.

Stahlman, P. W., and S. D. Miller. 1990. Downy brome (*Bromus tectorum*) interference and economic thresholds in winter wheat (*Triticum aestivum*). Weed Science 38:224–228.

Steinbauer, G. P., and B. H. Grigsby. 1957. Field and laboratory studies on the dormancy and germination of the seeds of chess (*Bromus secalinus* L.) and downy bromegrass (*Bromus tectorum* L.). Weeds 5:1–4.

Stewart, G., and A. C. Hull. 1949. Cheatgrass (*Bromus tectorum* L.)–an ecologic intruder in southern Idaho. Ecology 30:58–74.

Thill, D. C., K. George Beck, and R. H. Callihan. 1984. The biology of downy brome (*Bromus tectorum*). Weed Science 32:7–12.

Thornton, P. E., R. Shrestha, M. Thornton, S. C. Kao, Y. Wei, and B. E. Wilson. 2021. Gridded daily weather data for North America with comprehensive uncertainty quantification. Scientific Data 8:190.

Tran, N. H. T., D. Van Hoang, and L. T. Phan. 2024. Drought stress induces early flowering and the stress tolerance of offspring in *Petunia hybrida*. Plant Biotechnology 41:53–63.

Vahsen, M. L., T. M. Maxwell, D. M. Blumenthal, D. Gamba, M. J. Germino, M. B. Hooten, J. R. Lasky, E. A. Leger, N. Pirtel, L. M. Porensky, S. Romero, J. J. Van Ee, S. M. Copeland, D. J. Ensing, and P. B. Adler. 2025. Phenological sensitivity of *Bromus tectorum* genotypes depends on current and source environments. Ecology 106:e70025.

Valliant, M. T., R. N. Mack, S. J. Novak, M. O. T. V Alliant, R. I. N. M. Ack, S. T. J. N. Ovak, M. T. Valliant, R. N. Mack, and S. J. Novak. 2007. Introduction history and population genetics of the invasive grass *Bromus tectorum* (Poaceae) in Canada. American Journal of Botany 94:1156–1169.

Warg, S. A. 1938. Life history and economic studies on *Bromus tectorum*. PhD dissertation. University of Montana, Missoula, MT.

Werle, R., M. L. Bernards, T. J. Arkebauer, and J. L. Lindquist. 2014. Environmental triggers of winter annual weed emergence in the Midwestern United States. Weed Science 62:83–96.

Wicks, G. A. 1997. Survival of downy brome (*Bromus tectorum*) seed in four environments. Weed Science 45:225–228.

Zelikova, T. J., R. A. Hufbauer, S. C. Reed, T. Wertin, C. Fettig, and J. Belnap. 2013. Eco-evolutionary responses of *Bromus tectorum* to climate change: Implications for biological invasions. Ecology and Evolution 3:1374–1387.

Supporting Information

Appendix A. Phenology monitoring data used to calibrate and validate the DDRP model for BRTE. The geographic origin (State, Site, Latitude, and Longitude), phenological event description and corresponding code used in the model, year, date, day of year (DOY), and source

(Reference) of each observation. l0 = flowering, s0 = seed production, m0 = senescence, and s1 = seed germination.

Tables and Figures

Table 1. Summary of monitoring data used to calibrate and validate the phenology for *B. tectorum* (BRTE). Each observed event has a corresponding predicted event in the model. N_{loc}, number of locations; N_{obs}, number of observations.

Set	N_{site}	Years	N_{obs}	Event
calibration	14	2016, 2017, 2020, 2021, 2022	35	first flowering
calibration	3	2017, 2022	10	50% flowering
calibration	4	2022	4	first seed set
calibration	14	2016, 2017, 2020, 2021, 2022	41	first senescence
validation	21	2020, 2021, 2022	21	first flowering
validation	11	2021, 2022	11	first senescence

Table 2. DDRP parameter values for BRTE.

Parameter	Code	Value
Lower developmental threshold (°C)		
Seed	seedLDT	0
Seedling	seedlingLDT	0
Flower	flowerLDT	0
Mature	matureLDT	0
Upper developmental threshold (°C)		
Seed	seedUDT	35
Seedling	seedlingUDT	35
Flower	flowerUDT	35
Mature	matureUDT	35
Stage durations (°C degree-days)		
OWSeedling	OWseedlingDD	440
Seed	seedDD	1000
Seedling (not actually used for this annual plant)	seedlingDD	440
Flower	flowerDD	175
Mature	matureDD	315
Phenological events (°C degree-days)		
Seed event – suggested label “seed dormancy”	seedEventDD	172
Seedling event – suggested label “flowering”	seedlingEventDD	220
Flower event – suggested label “seed set”	flowerEventDD	175
Mature event – suggested label “senescence”	matureEventDD	315
Cold stress		
Cold stress temperature threshold (°C)	coldstress_threshold	–32
Cold degree-day (°C) limit when most individuals die	coldstress_units_max1	100
Cold degree-day (°C) limit when all individuals die	coldstress_units_max2	150
Heat stress		
Heat stress temperature threshold (°C)	heatstress_threshold	44
Heat stress degree-day (°C) limit when most individuals die	heatstress_units_max1	40
Heat stress degree-day (°C) limit when all individuals die	heatstress_units_max2	80
Dry stress		
Dry stress threshold ($m^3\ m^{-3}$)	drystress_threshold	0.02
Dry stress limit when most individuals die	drystress_units_max1	80
Dry stress limit when all individuals die	drystress_units_max2	100
Wet stress		
Wet stress threshold ($m^3\ m^{-3}$)	wetstress_threshold	0.92
Wet stress limit when most individuals die	wetstress_units_max1	4
Wet stress limit when all individuals die	wetstress_units_max2	8

Parameter	Code	Value
Cohorts		
Degree-days (°C) to complete seeding development (average)	distro_mean	555
Degree-days (°C) to complete seedling development (variation)	distro_var	10000
Minimum degree-days (°C) to complete seedling development	xdist1	425
Maximum degree-days (°C) to complete seedling development	xdist2	685
Shape of the distribution	distro_shape	normal
Other		
Order of stages	stgorder	OL, F, M, S, L
Obligate annual (1 = TRUE)	obligate_annual	1
Degree day calculation method	calctype	triangle

Table 3. Performance of candidate antecedent soil moisture metrics and antecedent periods for explaining variation in flowering prediction error for BRTE. Linear regressions were fitted between flowering prediction error (predicted minus observed day of year) and cumulative antecedent soil moisture (AUC) calculated from surface soil moisture, root-zone soil moisture, and the vertical soil moisture gradient over six antecedent periods (7–42 days before flowering). Model performance is summarized using the coefficient of determination (R^2), Akaike information criterion (AIC), and root mean square error (RMSE). The selected linear regression (bold font) was used for developing the moisture-modified degree-day model for the seedling stage (i.e., prior to flowering).

Window	Type	R^2	AIC	RMSE
7	root-zone	0.00	346.9	21.5
7	surface	0.21	337.8	19.0
7	gradient	0.52	318.7	14.8
14	root-zone	0.00	346.9	21.5
14	surface	0.21	337.8	19.1
14	gradient	0.47	323.1	15.7
21	root-zone	0.00	346.9	21.5
21	surface	0.21	338.2	19.1
21	gradient	0.47	322.5	15.6
28	root-zone	0.00	346.9	21.5
28	surface	0.21	337.9	19.1
28	gradient	0.52	318.8	14.8
35	root-zone	0.00	346.9	21.5
35	surface	0.22	337.4	19.0
35	**gradient**	**0.58**	**314.0**	**13.9**
42	root-zone	0.00	346.9	21.5
42	surface	0.22	337.5	19.0
42	gradient	0.59	313.4	13.8

Table 4. Performance of the moisture-modified DDRP model for BRTE that applied seven different values of the moisture sensitivity coefficient (*k*). Model performance was assessed using mean absolute error (MAE), root mean square error (RMSE), mean prediction bias, and the mean within-site standard deviation (SD) of prediction error across years. The selected value (bold font) minimized MAE while maintaining near-minimum within-site variability in prediction error.

k	MAE	RMSE	Bias	Mean within-site SD
0.20	14.4	18.3	–1.5	8.1
0.25	14.4	18.0	–2.0	8.0
0.30	14.1	17.5	–2.4	7.9
0.35	14.2	17.4	–2.7	7.9
0.40	**14.0**	**16.9**	**–3.3**	**7.5**
0.45	14.2	16.9	–3.5	7.4
0.55	14.5	17.2	–4.2	7.4

Table 5. Summary statistics for phenological events predicted by the phenology model for BRTE based on datasets used for model calibration and validation. The number of observations (N_{obs}), mean absolute error (MAE), bias with standard deviation (SD), and range of differences between predicted and observed dates (in days) are shown for each event. MAE = the average absolute difference of (predicted – observed), Bias = average of (predicted – observed), SD = standard deviation of (predicted – observed). Mean within-site SD (Site SD) is reported for the calibration datasets.

Set	Event	MAE	RMSE	Bias	Mean within-site SD
calibration	first flowering	13.6	16.3	−1.9	7.2
validation	first flowering	14.8	16.6	0.6	
calibration	50% flowering	9.9	11.5	−0.7	7.2
calibration	seed set	15.5	19.7	−2.5	
calibration	senescence	11.7	14.1	−0.1	7.7
validation	senescence	11.6	13.8	5.3	

Figure 1. Geographic distribution of BRTE phenological observations used to calibrate and validate the phenology model. Sites sampled over multiple years contributed to model calibration, whereas single-year observations were used for model validation. Point locations are slightly jittered for visualization purposes to reduce overlap among sites with multiple phenological events.

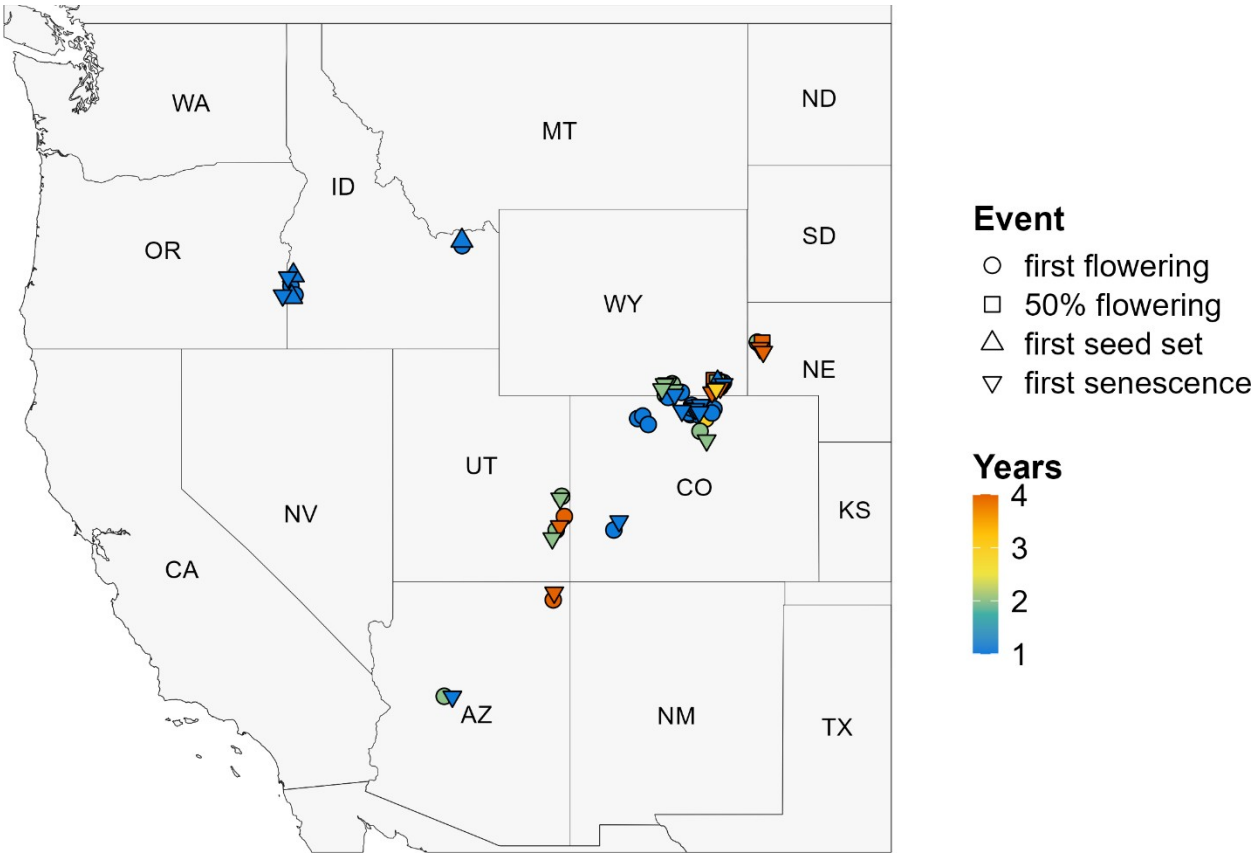

Figure 2. Results of the climate analysis of BRTE presence records using candidate thresholds for cold, heat, dry, and wet stress. Lines show the mean number of consecutive days (>0, >7, and >14 days) that presence locations exceeded each threshold value over a 20-year (temperature) or 10-year (soil moisture) period.

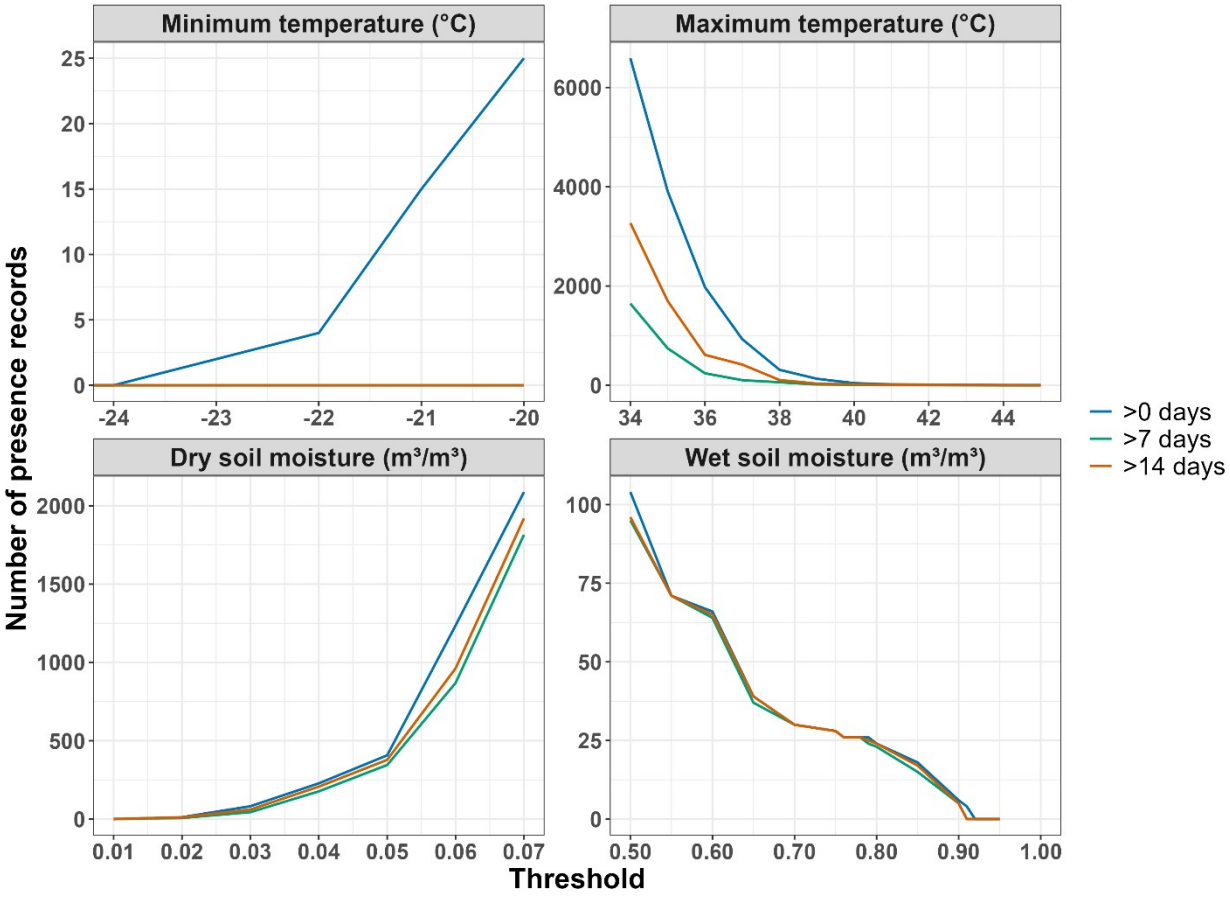

Figure 3. Relationship between the 35-day cumulative antecedent soil moisture gradient and flowering prediction error (predicted DOY – observed DOY) for the temperature-only phenology model for BRTE. Positive prediction errors indicate flowering was predicted too late, whereas negative values indicate flowering was predicted too early. The fitted regression line illustrates the association between the 35-day cumulative antecedent soil moisture conditions and systematic prediction error, providing the basis for incorporating a moisture modifier into daily degree-day accumulation.

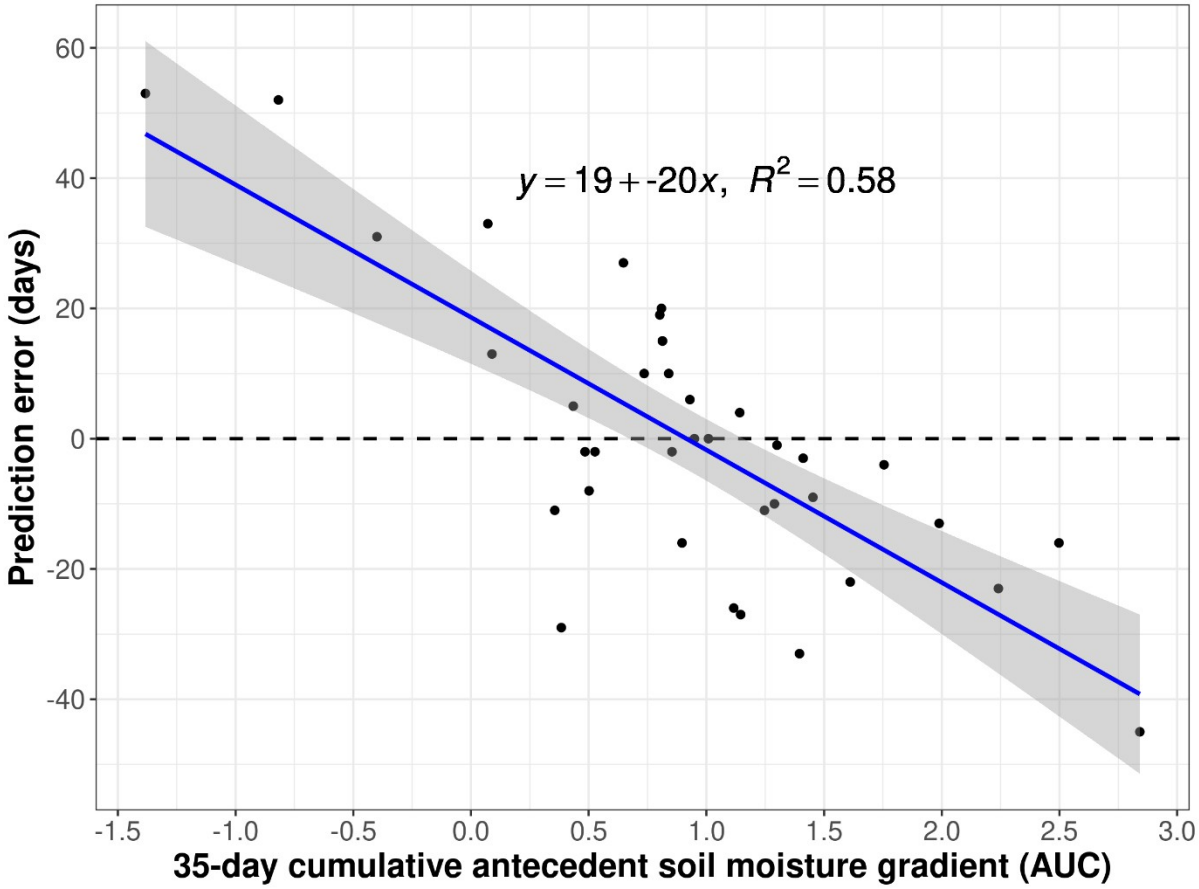

Figure 4. The modeled potential distribution for BRTE in North America (CONUS, southern Canada, and northern Mexico) according to DDRP runs for 10 recent years (2016−2025). Maps (A) and (B) are identical except for the depiction of the presence records used for model calibration in B. Yellow areas were included in the potential distribution for all years, whereas areas with cooler colors were excluded by moderate or severe climate stresses for ≥1 years.

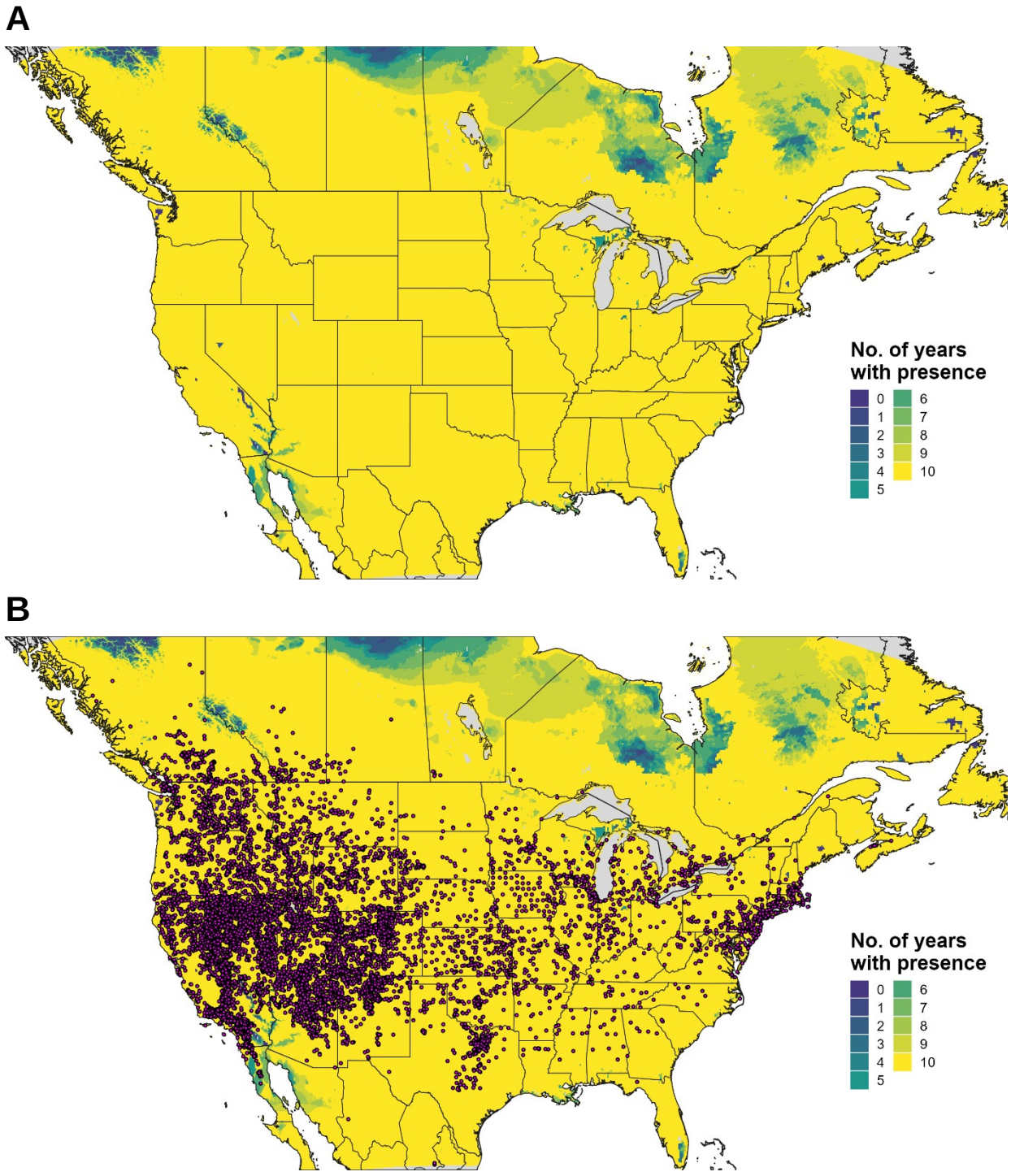

Figure 5. Average annual climate stress accumulations for BRTE across North America during 2016–2025, as predicted by DDRP. Maps show (A) cold, (B) heat, (C) dry, and (D) wet stress accumulations.

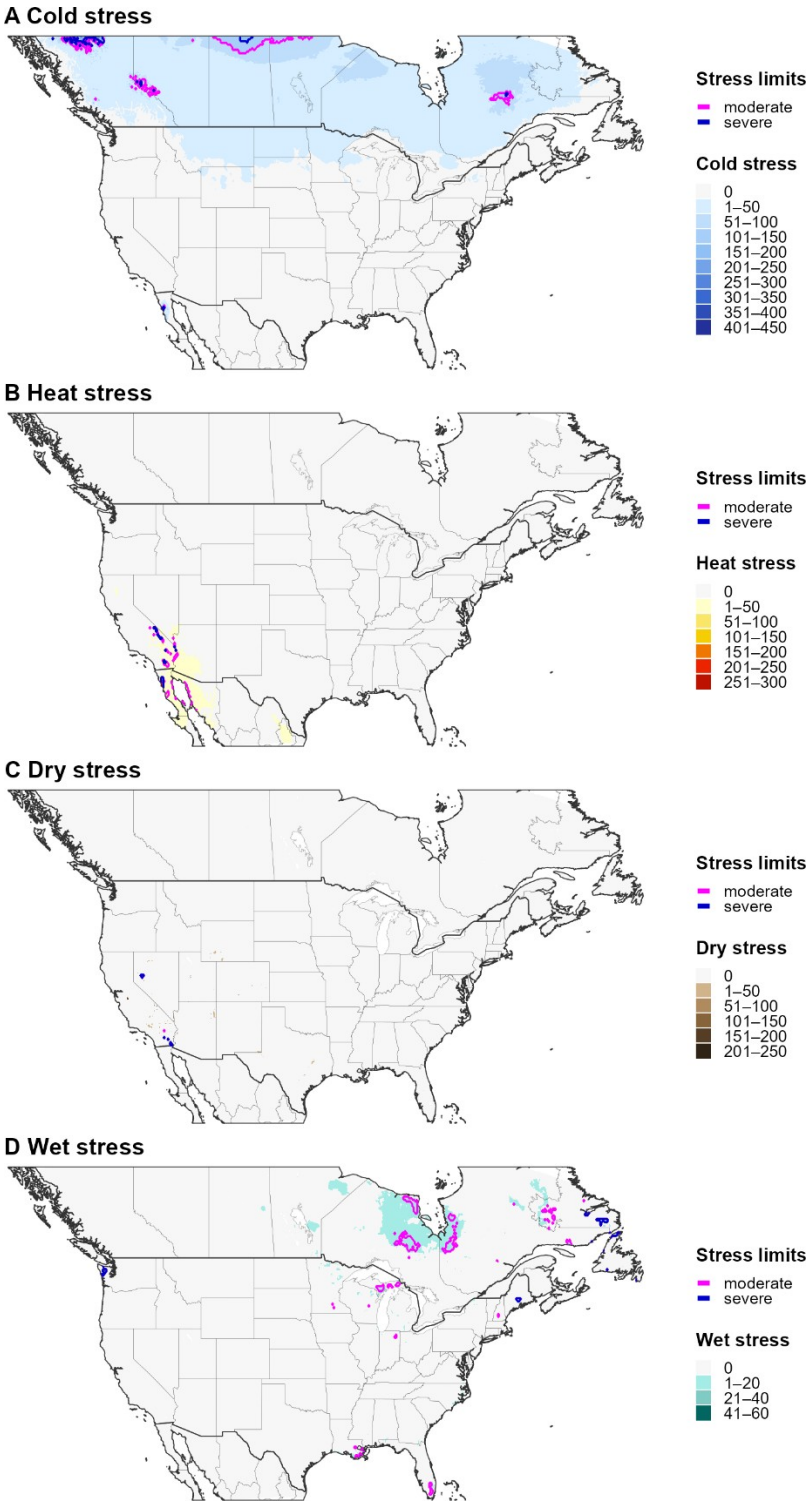

Figure 6. Maps of the predicted dates of first (A) flowering, (B) seed set, and (C) senescence of BRTE with severe and moderate climate stress exclusions (based on cold, heat, dry and wet stress units) for CONUS for 2024 produced by DDRP.

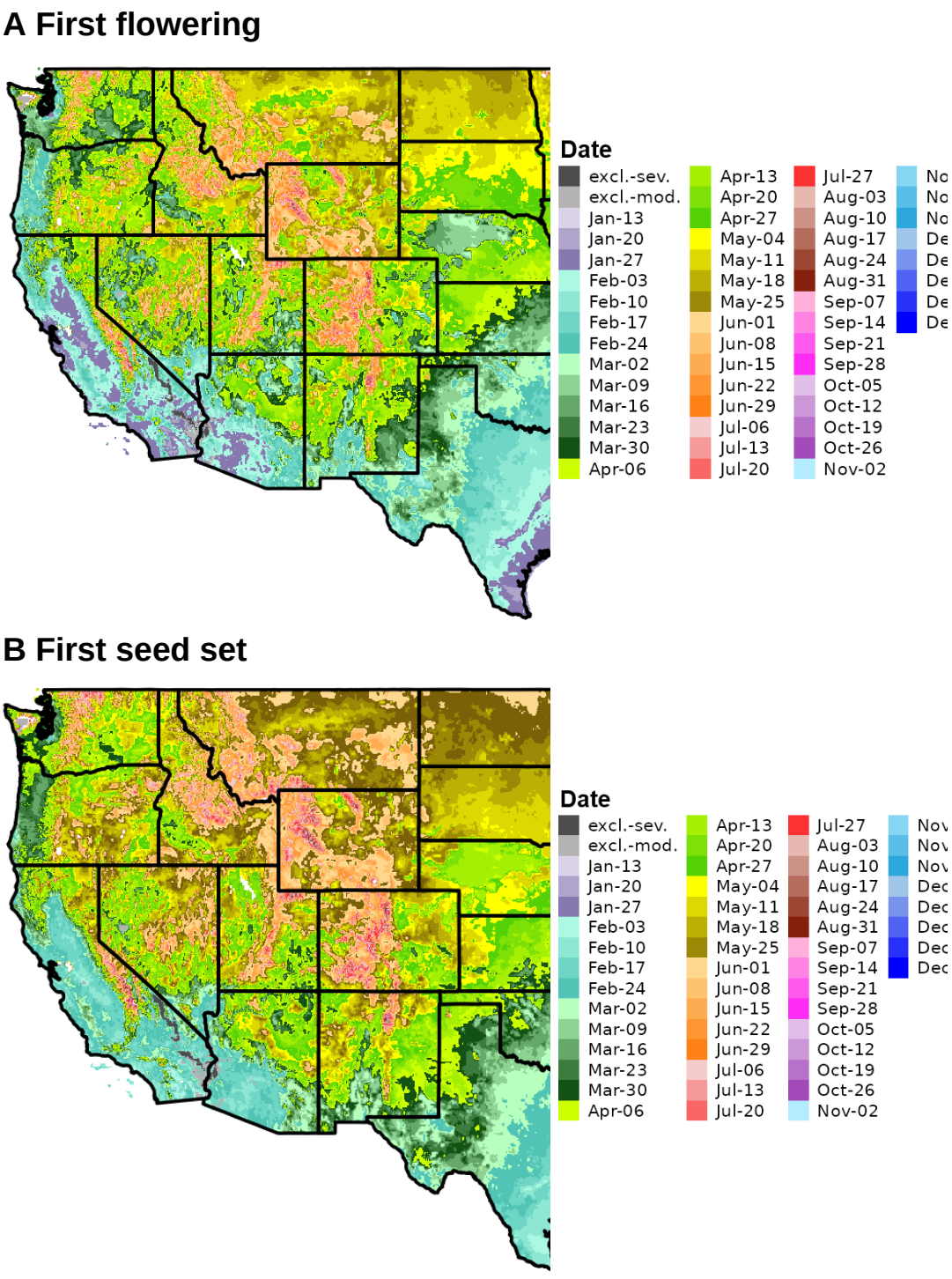

C First senescence